



ChemComm

**Synthesis of microporous polymers with exposed C<sub>60</sub> surface by polyesterification of fullerenol**

Journal:	<i>ChemComm</i>
Manuscript ID	CC-COM-02-2022-000728.R1
Article Type:	Communication

SCHOLARONE™  
Manuscripts

## COMMUNICATION

## Synthesis of microporous polymers with exposed C<sub>60</sub> surface by polyesterification of fullereneol

Received 00th January 20xx,  
Accepted 00th January 20xx

Hiroto Nishihara<sup>\*a, b</sup>, Akio Harigaya,<sup>b</sup> Alberto Castro Muniz,<sup>c</sup> Mao Ohwada,<sup>a</sup> Takashi Kyotani,<sup>b</sup> and Yuta Nishina<sup>\*d</sup>

DOI: 10.1039/x0xx00000x

**Microporous polymers with exposed C<sub>60</sub> surface have been synthesized by a new pathway of crosslinking fullereneol and terephthaloyl chloride or 1,3,5-benzenetricarbonyl trichloride via esterification. The resulting polymers are insoluble solids containing a large ratio of C<sub>60</sub> with hydroxy groups and possess micropores with high specific surface area up to 657 m<sup>2</sup> g<sup>-1</sup>. The microporous polymers thus obtained exhibit enhanced hydrogen spillover which is unique property of the C<sub>60</sub> surface.**

Fullerenes represented by C<sub>60</sub> are spherical molecular carbon allotropes which have many unique functions such as electron accepting ability,<sup>1</sup> catalysis,<sup>2, 3</sup> electrochemical activity,<sup>4</sup> and biochemical activity.<sup>5</sup> Although many of the fullerene functions are derived from its molecular surface, most of the molecular surface is hidden at solid-state fullerenes because of their close packing structures induced by relatively strong intermolecular forces. For example, the geometric surface area (outside surface only) of a single C<sub>60</sub> molecule can be calculated as 2625 m<sup>2</sup> g<sup>-1</sup> when its outside diameter is assumed as 1 nm considering the Van der Waals radius.<sup>6</sup> However, measured surface area of C<sub>60</sub> solid powder is almost 0 m<sup>2</sup> g<sup>-1</sup>. To fully enjoy the surface-derived functions of fullerenes, it is necessary to design fullerene-based porous frameworks, namely fullerene polymers, in which molecular surface of fullerene is exposed.

There have been many reports on the synthesis of fullerene polymers,<sup>7</sup> and they can be classified into two categories: 100% fullerene type and composite type. The former can be synthesized by subjecting C<sub>60</sub> solid to high pressure and high temperature.<sup>8, 9</sup> Despite their unique properties such as

photoluminescence<sup>10</sup> and magnetism,<sup>11</sup> they are dense solids with poor porosity. The latter category is further classified into several different types such as side chain, star shaped, and crosslinked,<sup>7</sup> and the crosslinked type is the most reasonable design to achieve our purpose. Traditionally, the crosslinked C<sub>60</sub> polymers were synthesized with the aim of their optical properties, and soluble polymers were appreciated.<sup>12-14</sup> More recently, insoluble and porous C<sub>60</sub> polymers has attracted interest. Bein *et al.* reported fullerene-based ordered mesoporous polymer, but the C<sub>60</sub> content was ca. 20 wt%.<sup>15</sup> Zhu *et al.* synthesized C<sub>60</sub>-rich porous aromatic frameworks by crosslinking C<sub>60</sub> with alkyl chains via AlCl<sub>3</sub> catalysed reaction, and achieved a high surface area of 1094 m<sup>2</sup> g<sup>-1</sup>.<sup>16</sup> Tan *et al.* used dihydronaphthyl-functionalized C<sub>60</sub> as a building block and synthesized microporous polymers with a high surface area of 753 m<sup>2</sup> g<sup>-1</sup>.<sup>17</sup> While these works have pioneered porous fullerene-based polymers, further extension of chemical diversity is desired for practical applications that require different properties depending on purposes. Herein, we report a new pathway of fullerene-based polymers with developed microporosity by using hydrophilic fullereneol (C<sub>60</sub>(OH)<sub>n</sub>) as a building block with aiming good dispersibility of the resulting polymer in polar solvent. Up to now, coordination polymer (222 m<sup>2</sup> g<sup>-1</sup>)<sup>18</sup> and hydrogen-bonding network (351 m<sup>2</sup> g<sup>-1</sup>)<sup>19</sup> based on fullereneol have been reported, but their surface areas were much lower than those of the above-mentioned polymers. Our strategy is to use terephthaloyl chloride (TC) or 1,3,5-benzenetricarbonyl trichloride (BT) as a crosslinker via esterification and synthesise rigid polyester frameworks with developed microporosity. Moreover, we examine the exposure of C<sub>60</sub> surface in the resulting polymer by measuring hydrogen spillover effect<sup>24</sup> to ensure the distinct surface property compared to conventional porous carbon materials.<sup>20-23</sup>

Fullereneol (C<sub>60</sub>(OH)<sub>n</sub>·mH<sub>2</sub>O) was purchased from Frontier Carbon Co., Ltd. The FT-IR spectrum of fullereneol (Fig. S1) indicates the presence of hydroxyl groups and a small amount of ketone structures derived from *vic*-diol moieties and hemiketal moieties, as Chiang *et al.* reported.<sup>25</sup> From the elemental composition shown in Table S1, the molar ratio of C<sub>60</sub>:H:O can be obtained as 1:20.7:14.6. Thus, *n* and *m* in

<sup>a</sup> Advanced Institute for Materials Research (WPI-AIMR), Tohoku University, 2-1-1 Katahira, Aoba-ku, Sendai, Miyagi, 980-8577, Japan.

<sup>b</sup> Institute of Multidisciplinary Research for Advanced Materials, Tohoku University, 2-1-1 Katahira, Aoba-ku, Sendai, Miyagi, 980-8577, Japan.

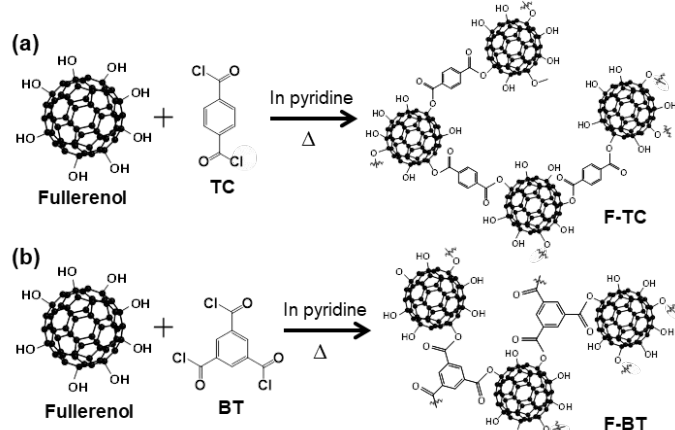
<sup>c</sup> Instituto del Ciencia y tecnología del Carbon, INCAR-CSIC, C/Francisco Pintado Fe 26, 33011 Oviedo, Spain.

<sup>d</sup> Research Core for Interdisciplinary Sciences, Okayama University, Tsushima-ku, Okayama 700-8530, Japan.

Email: hiroto.nishihara.b1@tohoku.ac.jp; nisina-y@cc.okayama-u.ac.jp

† Electronic Supplementary Information (ESI) available: Experimental details and additional characterization data. See DOI: 10.1039/x0xx00000x

$C_{60}(OH)_n \cdot mH_2O$  can be calculated as 8.5 and 6.1, respectively. The average number of hydrated water,  $m = 6.1$ , corresponds to 11 wt% in  $C_{60}(OH)_{8.5} \cdot 6.1H_2O$ , and it accords well with the estimation by TG (10 wt%, Fig. S2). Moreover, the average number of hydroxy groups ( $-OH$ ),  $n = 8.5$ , almost accords to the results of matrix-assisted laser desorption ionization time-of-flight mass spectrometry (MALDI-TOF-MS, Fig. S3). Two kinds of fullerene-based polymers (F-TC and F-BT) were synthesized by esterification between fullereneol and crosslinker (TC or BT), respectively, in accordance with Scheme 1. The polymerization was performed by heating the mixture with a microwave reactor (Anton Paar, Monowave 300), typically at 180 °C for 1 h. The detailed procedure is described in the Supporting Information. By changing the molar ratio of crosslinker/fullereneol, fullerene-based polymers listed in Table 1 were synthesized. The stoichiometric fraction of  $C_{60}$  included in F-TC and F-BT can be estimated as 56.3 and 52.6%, when the  $CL/C_{60}(OH)_{8.5}$  ratios are 2.5 and 2.2, respectively.



**Scheme 1** Synthesis of fullerene-based polymers using (a) TC and (b) BT as crosslinkers.

**Table 1** Synthesis conditions and the properties of fullerene-based polymers.

Polymer	CL/ $C_{60}(OH)_{8.5}$ molar ratio <sup>a</sup>	Yield <sup>b</sup> (%)	$S_{BET}$ <sup>c</sup> ( $m^2 g^{-1}$ )
F-TC	0.53	60.0	657
F-TC	1.1	48.4	640
F-TC	2.5	48.1	503
F-TC	4.3	39.3	520
F-BT	2.2	47.6	559
F-BT	4.4	32.6	541

<sup>a</sup> Molar ratio of crosslinker (CL; TC or BT) over  $C_{60}(OH)_{8.5}$  calculated from their weights used for the polymer synthesis. <sup>b</sup> The mass ratio of fullerene polymer based on the total mass of reactant (CL and  $C_{60}(OH)_{8.5}$ ). <sup>c</sup> BET surface area.

To estimate the efficiency of polymerization, the yield of fullerene-based polymer was calculated by dividing the dry-based polymer mass (g) by the mass (g) of reactants (the sum of crosslinker and fullereneol). Note that the measured mass of fullereneol was converted into a molar amount using  $C_{60}(OH)_{8.5} \cdot 6.1H_2O$ , and the corresponding mass of  $C_{60}(OH)_{8.5}$  (monomer excluding hydrated water) was used for the yield

calculation. If all of crosslinker and fullereneol are reacted into insoluble polymer, a yield becomes 100%. However, as shown in Table 1, the yields of the fullerene-based polymers are much less than 100%. This is ascribed to the presence of fullereneol molecules with very small amount of  $-OH$  groups (Fig. S3). It causes a termination of polymerization, where a crosslinker or a fullereneol molecule can bind to only one molecule. Regarding the reactant composition, it is found that the yields of both types of polymers become larger when the ratio of crosslinker is decreased. This suggests that the amount of crosslinker is excessive for the polymers synthesized by the large crosslinker/fullereneol ratio. Since one crosslinker is shared by two fullereneol molecules, the crosslinker/fullereneol ratio of 4.4 corresponds to 8.8 crosslinkers attached to one fullereneol molecule, but it seems to be difficult to achieve such a structure because of steric hindrance as well as limited number of  $-OH$  groups in some fullereneol molecules (Fig. S3).

Fig. 1a shows the FT-IR spectra of fullereneol, crosslinkers, and fullerene-based polymers. Fullereneol shows four broad bands of  $\nu O-H$  ( $3400\text{ cm}^{-1}$ ),  $\nu C=C$  ( $1619\text{ cm}^{-1}$ ),  $\delta_s C-O-H$  ( $1385\text{ cm}^{-1}$ ), and  $\nu C-O$  ( $1051\text{ cm}^{-1}$ ) as typically found in literature.<sup>25-27</sup> In the fullerene-based polymers,  $\nu O-H$  and  $\delta_s C-O-H$  bands are weakened, while  $\nu C=C$  and  $\nu C-O$  bands are retained. Moreover, a new band corresponding to a C-O stretching of ester ( $\nu C(=O)-O$ ) appears at  $1272\text{ cm}^{-1}$ . These spectra changes accord well with the polymerization reactions shown in Scheme 1. We have confirmed that the fullerene-based polymers are insoluble in water, ethanol, acetone, and pyridine. Moreover, even if the polymer was immersed in dimethyl sulfoxide- $d_6$  and heat treated at 100 °C for 3 h, no fragmentation was observed by  $^1H$ -NMR (Fig. S4). Thus, the fullerene-based polymers synthesized in this work have a good stability against a variety of solvent, and it is important for adsorbent applications.

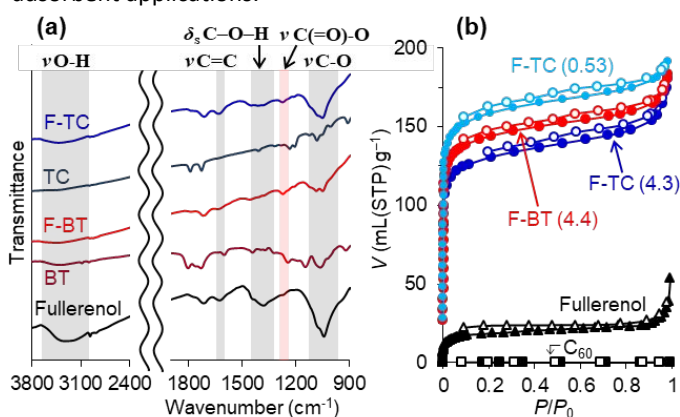


**Figure 1** (a) FT-IR spectra of fullereneol, BT, TC, and fullerene-based polymers. Four major bands of fullereneol are highlighted by gray bars, while a C-O stretching band of ester is highlighted by a red bar. (b)  $N_2$  adsorption-desorption isotherms of  $C_{60}$ , fullereneol, F-TC, and F-BT measured at  $-196\text{ }^\circ\text{C}$ . CL/ $C_{60}(OH)_{8.5}$  ratios of polymers are shown in parenthesis.

The chemical forms of carbon in the fullerene-based polymer were further analysed by X-ray photoelectron microscopy (XPS), as shown in Fig. S5 and Table S2. There are three carbon forms:  $C=C/C-C$  in polymer backbone (88.5%), C-O corresponding to

remaining hydroxy groups (5.7%), and O=C=O corresponding to ester moiety (5.8%). From the XPS results, the numbers of remaining hydroxy groups and crosslinkers attached to fullerene were estimated to 4.4 and 4.6 per one C<sub>60</sub>, respectively. The retention of hydroxy groups makes the polymer hydrophilic, and it is advantageous for preparing polymer paste with water-based solvent in practical applications. The number of crosslinker attached to one C<sub>60</sub> unit (4.6) is reasonable to develop microporosity in the polymer.

The porosity of the fullerene-based polymers was examined by N<sub>2</sub> adsorption-desorption measurement (Fig. 1b). Prior to the measurement, the polymer was degassed at 150 °C that is below thermal decomposition temperature confirmed by TG measurement coupled with mass spectroscopy (Fig. S6). Note that evacuation at 150 °C is popularly used to eliminate physisorbed water from porous carbon materials without decomposition of oxygen-functional groups such as hydroxy and carboxy groups.<sup>28</sup> For comparison, the data of fullerene C<sub>60</sub> and fullerenol are shown together. Fullerene C<sub>60</sub> forms a fcc crystal and its powder shows a completely non-porous behaviour. Thus, its measured Brunauer-Emmett-Teller (BET) surface area ( $S_{\text{BET}}$ ) is 0 m<sup>2</sup> g<sup>-1</sup>. Fullerenol shows a small amount of N<sub>2</sub> adsorption, and its  $S_{\text{BET}}$  is 110 m<sup>2</sup> g<sup>-1</sup>. By contrast, both F-TC and F-BT polymers exhibit a large amount of N<sub>2</sub> adsorption amount. The isotherms are classified as Type I which is typical for microporous solids with the pore size less than 2 nm.<sup>29</sup> Indeed, the pore-size distribution of F-TC, which was calculated by the non-local density functional theory,<sup>30</sup> shows a sharp peak at 0.55 nm (Fig. S7).  $S_{\text{BET}}$  of the resulting polymer is up to 657 m<sup>2</sup> g<sup>-1</sup>, much higher than those of the reported coordination polymer (222 m<sup>2</sup> g<sup>-1</sup>)<sup>18</sup> and hydrogen-bonding network (351 m<sup>2</sup> g<sup>-1</sup>)<sup>19</sup> consisting of fullerenol. The presence of micropores in the fullerene-based polymers strongly suggests that inter-fullerene spaces are created by the insertion of crosslinkers.

The structural details of the F-BT polymer were analysed by observations with scanning electron microscopy (SEM) and transmission electron microscopy (TEM). As shown in Fig. S8a, commercial fullerene is a powder with relatively large particle size (2–10 μm). Fullerenol is first completely dissolved in pyridine, and a polymer is precipitated as fine powder with much smaller particle size of 100–500 nm after polyesterification (Fig. S8b). Its TEM image (Fig. 2a) shows dense polymer framework. A high magnification image (Fig. 2b) displays relatively uniform-sized micropores (white dots) inside the polymer. As reference, TEM images of conventional porous carbon materials (activated carbon fiber and Ketjenblack) are shown in Fig. S9. Conventional porous carbons consist of graphene sheets and slit-shaped micropores exist between the graphene sheets. The structure of F-BT (Fig. 2b) is clearly different from those of conventional porous carbon materials. There is no graphene sheet structure and the micropores are formed as inter-fullerene spaces rather than slit-shaped micropores between graphene sheets.

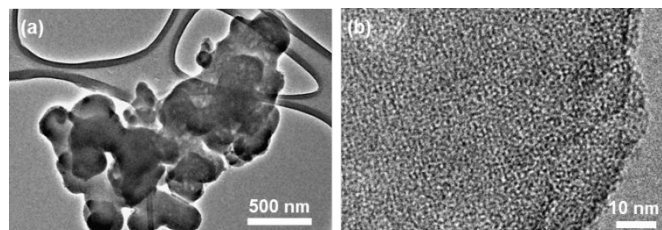


**Figure 2** TEM images of F-BT at (a) low and (b) high magnifications.

The results shown above suggest that the fullerene-based polymers synthesized in this work contain exposed molecular surface of C<sub>60</sub>. To examine the C<sub>60</sub>-derived surface property, we demonstrate the enhancement of hydrogen spillover.<sup>31–33</sup> It is well known that H<sub>2</sub> is dissociatively chemisorbed onto the Pt surface, and the resulting atomic H (H radical) migrates to a Pt support.<sup>20, 32</sup> The migration is called hydrogen spillover. Depending on the property of graphene-based support, the measured migration amount differs. It has been reported that curved graphene surface<sup>32</sup> and C<sub>60</sub> surface<sup>24</sup> exhibit enhanced hydrogen spillover amount. Thus, the observation of the enhanced hydrogen spillover can prove the exposure of the C<sub>60</sub> surface in the fullerene-based polymers.

1 wt% of Pt nanoparticles (2–3 nm) are loaded onto F-BT by simply mixing commercial Pt nanocolloid solution with F-BT. A TEM image of the resulting Pt-loaded F-BT (denoted as Pt/F-BT) is shown in Fig. 3a. Since the pore size of fullerene-based polymers is less than 2 nm, Pt nanoparticles should be dispersed outside of polymer particles. We have previously demonstrated that such a loading condition is valid for observing hydrogen spillover via the loading of the same Pt nanoparticle onto an ordered microporous carbon with the pore size of 1.2 nm.<sup>32</sup> As a reference, typical porous carbon support (ketjenblack, KB, EC600JD, Lion) and its Pt-loaded sample which was previously reported<sup>24</sup> (denoted as Pt/KB, Pt-loading amount is 0.9 wt%, Fig. 3b) is used. H<sub>2</sub> adsorption-desorption isotherms measured on Pt/F-BT are shown in Fig. S10. We have previously established a reliable protocol to evaluate hydrogen spillover effect from precise and reproducible H<sub>2</sub> adsorption-desorption measurement where proper pre-treatment conditions and measurement conditions were carefully determined.<sup>32</sup> Pt/F-BT exhibits very large H<sub>2</sub> uptake at the 1<sup>st</sup> measurement, whereas the uptake amount is decreased later on and becomes almost constant after the 3<sup>rd</sup> measurement. Such behaviour indicates that an irreversible hydrogenation takes place at the 1<sup>st</sup> and the 2<sup>nd</sup> measurement, and the polymer surface becomes stable after the 3<sup>rd</sup> measurement. Thus, the 4<sup>th</sup> measurement result on Pt/F-BT is compared with H<sub>2</sub> adsorption-desorption isotherms of F-BT in Fig. 3c. The reference data on KB and Pt/KB are taken from the literature.<sup>24</sup> KB is comprised of graphene sheets, and its surface can be considered as flat counterpart against the curved C<sub>60</sub> surface. Both in F-BT and KB, H<sub>2</sub> adsorption amount significantly increases after Pt loading, and the adsorption amount can be considered as the sum of chemisorption amount ( $M_0$ ) and pressure-dependent spillover amount [ $M_{\text{spill}}(P)$ ] in addition to the physisorption amount [ $M_{\text{phys}}(P)$ ] (Fig. S11).<sup>32</sup> The  $M_0$  values of Pt/F-BT and Pt/KB are comparable, indicating that the Pt surface areas of these samples are almost the same. According to the procedure which we have developed,<sup>32</sup> we calculated  $M_{\text{spill}}(P)$  as shown in Fig. 3d. Compared to Pt/KB, Pt/F-BT shows enhanced  $M_{\text{spill}}(P)$  despite its lower  $S_{\text{BET}}$  (Table S3). This can be ascribed to the curved C<sub>60</sub> surface which can strongly attract migrated H.<sup>24</sup> Indeed, the hydrogen spillover amount on F-BT is just in between the values of KB and C<sub>60</sub><sup>24</sup> as well as curved graphene framework (Table 4).<sup>32</sup> Thus, the fullerene-based polymers are

expected to be used as a new type of nanoporous materials with  $C_{60}$  surface properties such as radical capture and specific catalysis.

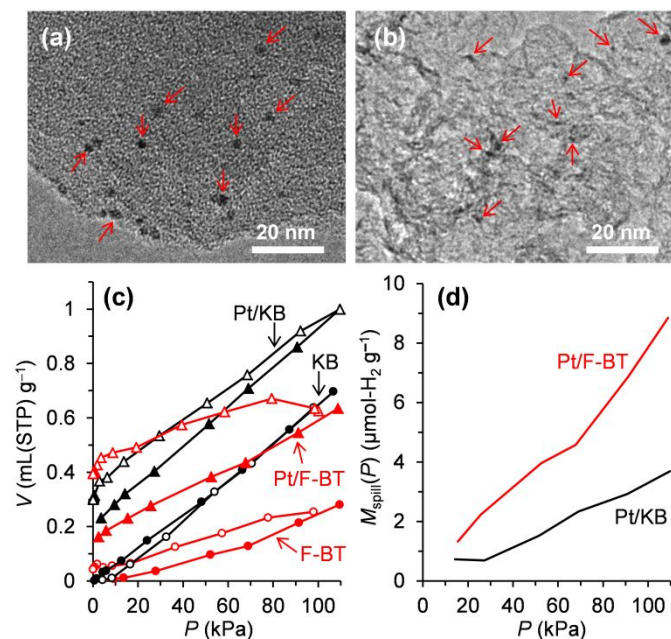


**Figure 3** (a,b) TEM images of (a) Pt/F-BT and Pt/KB. Platinum nanoparticles are indicated by arrows. (c) H<sub>2</sub> adsorption-desorption isotherms of F-BT, Pt/F-BT, KB, and Pt/KB measured at 25 °C. (d) Net spillover storage amount in Pt/F-BT and Pt/KB at 25 °C. Note that the spillover hydrogen uptake is expressed by the corresponding amount of H<sub>2</sub>, and its unit is μmol-H<sub>2</sub> g<sup>-1</sup>. The data of KB and Pt/KB are taken from the literature.<sup>24</sup>

In conclusion, microporous fullerene-based polymers were successfully synthesized by esterification of fullerenol and acid chloride. The fullerene-based polymers possess high surface area over 500 m<sup>2</sup> g<sup>-1</sup>, and exhibit enhanced hydrogen spillover which is unique property of the fullerene surface. This work was supported by JST CREST Grant no. JPMJCR118R3; JST SICORP Grant Number JPMJSC2112; the "Five-star Alliance" in "NJRC Mater. & Dev."; Japan Association for Chemical Innovation.

## Conflicts of interest

There are no conflicts to declare.

## Notes and references

- P. M. Allemand, A. Koch, F. Wudl, Y. Rubin, F. Diederich, M. M. Alvarez, et al., *J. Am. Chem. Soc.*, 1991, **113**, 1050-1051.
- B. Li and Z. Xu, *J. Am. Chem. Soc.*, 2009, **130**, 16380-16382.
- M. Nakaya, Y. Kitagawa, S. Watanabe, R. Teramoto, I. Era, M. Nakano, et al., *Adv. Sustain. Syst.*, 2021, **5**, 2000156.
- R. M. Giron, J. Marco-Martinez, S. Bellani, A. Insuasty, H. C. Rojas, G. Tullii, et al., *J. Mater. Chem. A*, 2016, **4**, 14284-14290.

- H. Tokuyama, S. Yamago, E. Nakamura, T. Shiraki and Y. Sugiura, *J. Am. Chem. Soc.*, 1993, **115**, 7918-7919.
- H. Nishihara and T. Kyotani, *Chem. Commun.*, 2018, **54**, 5648-5673.
- F. Giacalone and N. Martin, *Chem. Rev.*, 2006, **106**, 5136-5190.
- Y. Iwasa, T. Arima, R. M. Fleming, T. Siegrist, O. Zhou, R. C. Haddon, et al., *Science*, 1994, **264**, 1570-1572.
- R. Moret, T. Wågberg and B. Sundqvist, *Carbon*, 2005, **43**, 709-716.
- I. O. Bashkin, A. N. Izotov, A. P. Moravsky, V. D. Negrii, R. K. Nikolaev, Y. A. Ossipyan, et al., *Chem. Phys. Lett.*, 1997, **272**, 32-37.
- A. N. Andriotis, M. Menon, R. M. Sheetz and L. Chernozatonskii, *Phys. Rev. Lett.*, 2003, **90**, 026801.
- C. E. Bunker, G. E. Lawson and Y.-P. Sun, *Macromolecules*, 1995, **28**, 3744-3746.
- T. Cao and S. E. Webber, *Macromolecules*, 1996, **29**, 3826-3830.
- Y.-P. Sun, G. E. Lawson, C. E. Bunker, R. A. Johnson, B. Ma, C. Farmer, et al., *Macromolecules*, 1996, **29**, 8441-8448.
- N. K. Minar, K. Hou, C. Westermeier, M. Doblinger, J. Schuster, F. C. Hanusch, et al., *Angew. Chem. Int. Ed.*, 2015, **54**, 7577-7581.
- Y. Yuan, P. Cui, Y. Tian, X. Zou, Y. Zhou, F. Sun, et al., *Chem. Sci.*, 2016, **7**, 3751-3756.
- C. Zhang, S. Wang and B. Tan, *Chem. Commun.*, 2017, **53**, 12758-12761.
- Y. Wang, D. Nepal and K. E. Geckeler, *J. Mater. Chem.*, 2005, **15**, 1049-1054.
- S. Uchikawa, A. Kawasaki, N. Hoshino, T. Takeda, S. Noro, K. Takahashi, et al., *J. Phys. Chem. C*, 2019, **123**, 23545-23553.
- H. Nishihara and T. Kyotani, *Adv. Mater.*, 2012, **24**, 4473-4498.
- H. Itoi, H. Nishihara, T. Kogure and T. Kyotani, *J. Am. Chem. Soc.*, 2011, **133**, 1165-1167.
- H. Nishihara, T. Simura, S. Kobayashi, K. Nomura, R. Berenguer, M. Ito, et al., *Adv. Funct. Mater.*, 2016, **26**, 6418-6427.
- S. Sunahiro, K. Nomura, S. Goto, K. Kanamaru, R. Tang, M. Yamamoto, et al., *J. Mater. Chem. A*, 2021, **9**, 14296-14308.
- H. Nishihara, T. Simura and T. Kyotani, *Chem. Commun.*, 2018, **54**, 3327-3330.
- L. Y. Chiang, R. B. Upasani, J. W. Swirczewski and S. Soled, *J. Am. Chem. Soc.*, 1993, **115**, 5453-5457.
- F. F. Wang, N. Li, D. Tian, G. F. Xia and N. Xiao, *ACS Nano*, 2010, **4**, 5565-5572.
- X. Yang, M. Zhen, G. Li, X. Liu, X. Wang, C. Shu, et al., *J. Mater. Chem. A*, 2013, **1**, 8105-8110.
- H. Nishihara, Q. H. Yang, P. X. Hou, M. Unno, S. Yamauchi, R. Saito, J. I. Paredes, A. Martinez-Alonso, J. M. D. Tascon, Y. Sato, M. Terauchi, T. Kyotani, *Carbon*, 2009, **47**, 1220-1230.
- T. Matthias, K. Katsumi, V. N. Alexander, P. O. James, R.-R. Francisco, R. Jean, et al., *Pure Appl. Chem.*, 2015, **87**, 1051-1069.
- K. Chida, T. Yoshii, K. Takahashi, M. Yamamoto, K. Kanamaru, M. Ohwada, V. Deerattrakul, J. Maruyama, K. Kamiya, Y. Hayasaka, M. Inoue, F. Tani, H. Nishihara, *Chem. Commun.*, 2021, **57**, 6007-6010.
- H. Nishihara, P. X. Hou, L. X. Li, M. Ito, M. Uchiyama, T. Kaburagi, et al., *J. Phys. Chem. C*, 2009, **113**, 3189-3196.
- H. Nishihara, S. Ittisanronnachai, H. Itoi, L. X. Li, K. Suzuki, U. Nagashima, et al., *J. Phys. Chem. C*, 2014, **118**, 9551-9559.
- H. Nishihara, F. Ohtake, A. Castro-Muniz, H. Itoi, M. Ito, Y. Hayasaka, et al., *J. Mater. Chem. A*, 2018, **6**, 12523-12531.